
Commensurable spin structures and their excitations

A. R. Mackintosh and J. Jensen

15.1. Introduction

The standard model of rare-earth magnetism was constructed during the 1950s and early 1960s, and Roger Elliott was one of its major architects. One of the first coherent descriptions of the theory is to be found in his classic discussion of the magnetic structures of the heavy rare-earth metals by means of the molecular-field approximation (Elliott 1961). With his colleagues, he also gave in the following year an account of the magnetic excitations (Cooper *et al.* 1962). In these, as in other early theoretical treatments of rare-earth magnetism, most of the results were obtained by analytical means, and the problems caused by the incommensurability of the lattice and magnetic periodicities were either ignored or treated by perturbation theory. In this chapter we shall adopt a mean-field method which is closely related to those used earlier, but differing from them in two important respects. There is convincing experimental evidence that the periodicity of magnetic structures such as the helix in the rare earths (and particularly in holmium which we shall be considering in some detail) tends to 'lock in' to some rational multiple of the lattice periodicity. We have therefore studied such *commensurable* periodic structures, which have translational symmetry even though the period may be very long. This symmetry is utilized in *numerical* self-consistent mean-field calculations of the structures and, by a time-dependent extension of the method (the random-phase approximation), of the excitations. This procedure has allowed us to obtain detailed solutions under a variety of physical conditions, and has revealed features in both the structures and excitations which were not suspected until recently.

In the next section, we shall briefly describe the standard model and the way in which the mean-field calculations are performed. The method is applied to a discussion of spin-slip structures, whose salient features are described and related to the form of the magnetic interactions. A comparison is made between the calculated structures and those deduced from neutron diffraction measurements. The decisive role of the

hexagonal anisotropy is emphasized, and its decreasing importance with increasing temperatures illustrated. We then turn to a consideration of the dependence of the magnetic structure of holmium on magnetic field. We find that the puzzling 'extra' phases which have been observed in magnetization, magnetoresistance, and neutron-diffraction measurements can be explained by a new type of intermediate structure which we call a helifan. Comparison is made between the calculated structures and magnetization curves and those determined experimentally, and it is shown that the particular helifan which is observed depends on the way in which the experiment is performed. It is demonstrated that the occurrence of helifan structures depends on the form of the exchange, and that they tend to be suppressed by the hexagonal anisotropy. The excitations of commensurable periodic structures are finally considered and various effects due to the large hexagonal anisotropy in holmium are described. The excitations of structures with zero and increasing numbers of spin slips are discussed, and the experimental results which have so far been obtained on such structures are briefly summarized.

15.2. Spin-slip structures

We have calculated the magnetic structures of holmium as a function of temperature and magnetic field by means of the numerical self-consistent mean-field method developed by Jensen (1976). The measurements of Gibbs *et al.* (1985) have demonstrated that the periodicity of the helix in holmium tends to lock into the lattice period, and we have therefore performed our calculations on such commensurable structures, allowing for the distortions produced by the large hexagonal anisotropy and a possible field. Our starting point is the model used earlier by Larsen *et al.* (1987) to describe the structure and excitations in holmium at low temperatures. The Hamiltonian is

$$\mathcal{H} = \sum_{im} B_i^m O_i^m(\mathbf{J}_i) - \frac{1}{2} \sum_{ij} \sum_{\alpha\beta} \mathcal{J}^{\alpha\beta}(ij) J_{\alpha i} J_{\beta j} - g\mu_B \sum_i \mathbf{J}_i \cdot \mathbf{H}.$$

The first term is the single-ion crystal-field contribution, involving the Stevens operators O_i^m . The crystal-field parameters B_i^m were determined primarily from the magnetic structures and magnetization curves at low temperatures and remain unchanged throughout the calculation, although the effective anisotropy decreases with increasing temperature, roughly as $\sigma^{l(l+1)/2}$, due to the temperature-dependence of $\langle O_i^m \rangle$. The second term, the two-ion coupling, comprises an isotropic Heisenberg exchange and the dipolar interaction. The initial values for the former were taken from an earlier analysis of the spin waves in holmium (Jensen

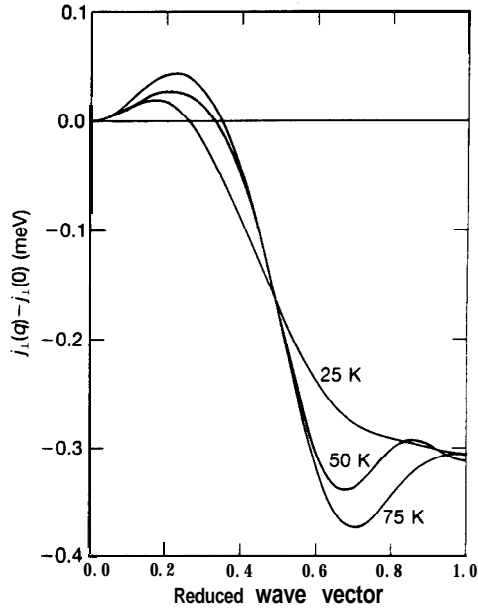


FIG. 15.1. The Fourier transforms, for wave vectors along the c -axis, of the exchange functions used in the calculations at different temperatures. It is noteworthy that the maximum increases in magnitude and moves to larger wave vector with increasing temperature. These functions, together with the crystal-field parameters B_i^m and the dipolar coupling, determine the calculated magnetic structures and excitations for holmium.

1988), and depend explicitly on the temperature, as shown in Fig. 15.1. They were adjusted slightly during the calculation, to reproduce correctly the transition fields from the helical phase, but remained consistent with the spin-wave data, within the experimental error.

Holmium crystallizes in the hcp structure and the atomic moments in any hexagonal plane are all aligned. The first step in the calculation is to assume a distribution $\langle \mathbf{J}_i \rangle$ of the moments at a given temperature. The structure is assumed commensurate with a repeat distance, deduced from experimental data, which may be as high as 50-100 atomic layers for the more complex configurations. The assumed values of $\langle \mathbf{J}_i \rangle$ are inserted into the Hamiltonian and a new set of moments calculated, using the mean-field method to reduce the two-ion term to the single-ion form. This procedure is repeated until self-consistency is attained. The free energy and the net moment in the field direction can then readily be calculated for the self-consistent structure.

The results of such self-consistent calculations for different temperatures and commensurate periodicities are shown in Fig. 15.2. At 4 K the large

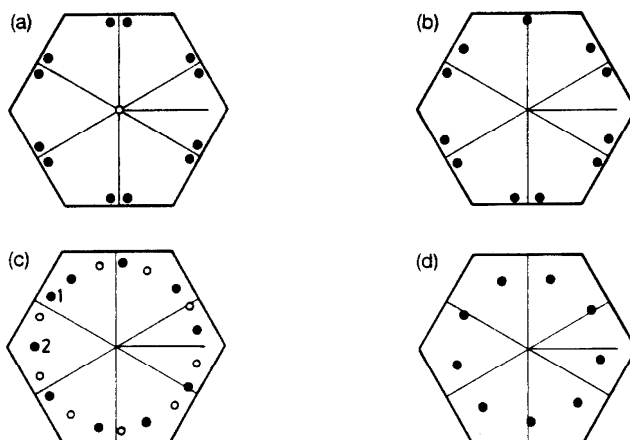


FIG. 15.2. The self-consistent periodic structures calculated at different temperatures. Each circle represents the magnitude and direction of the ordered moment in a specific plane, relative to the size of the moment at absolute zero ($10\mu_B$), indicated by the length of the horizontal lines. The orientation of moments in adjacent planes is depicted by the positions of neighbouring circles. (a) The 12-layer zero-spin-slip structure at 4 K. The open circle in the centre indicates the ferromagnetic component in the cone structure. (b) The 11-layer one-spin-slip structure at 25 K. The bunched pairs of moments are disposed unsymmetrically with respect to the easy axis in the vicinity of the spin-slip. (c) The 19-layer structure at 50 K. The orientation of the moments in successive layers is determined by following first the filled circles in an anticlockwise direction, as indicated, and then the open circles. (d) The 9-layer trigonal structure at 75 K. This may be looked upon as a three-spin-slip structure, but the bunching is so slight that it is more appropriate to regard it as an almost regular helix in which every third plane aligns its moments close to an easy axis in order to reduce the anisotropy energy.

hexagonal anisotropy causes the moments to bunch around the easy directions of magnetization so that the angle ϕ between any moment and the nearest b -axis is only 5.8 degrees, compared with the 15 degrees which corresponds to a uniform helix. As the temperature is increased the expectation value $\langle O_6^6 \rangle$ decreases with the relative magnetization roughly like σ^{21} and ϕ increases correspondingly. Simultaneously Q tends to increase so that the structure at 25 K has reduced its periodicity to 11 layers by introducing a regularly-spaced series of spin-slips, at which one plane of a bunched doublet is omitted while the remaining member orients its moments along the adjacent easy axis. The configuration of Fig. 15.2(b), in which one spin-slip is introduced for each repeat distance of the perfect commensurable structure, is the primordial spin-slip structure and has a number of interesting features. It is particularly stable,

existing over a range of temperature (Gibbs *et al.* 1985), possesses a net moment, and the bunching angle is still rather small. Although the angle 2ϕ between two bunched planes is almost constant, the exchange interaction distorts the structure near the spin-slips so that the moments are not symmetrically disposed around the easy axis. As the temperature is increased further, the bunching decreases and the concept of spin-slips becomes less useful. Thus the configuration of Fig. 15.2(d) can be considered as a three spin-slip structure, but it is simpler to regard it as a commensurate, almost regular helix in which every third plane aligns its moments close to an easy axis in order to reduce the anisotropy energy.

The spin-slip structures of holmium have been subjected to careful neutron-diffraction study by Cowley and Bates (1988). They interpreted their results in terms of three parameters:

- b , the number of lattice planes between spin-slips;
- 2α , the average angle between the moments in a bunched pair;
- σ , a Gaussian-broadening parameter for α .

In a perfect, undistorted structure, $\alpha = \phi$ and $\sigma = 0$. The parameter σ takes into account two effects; the distortions which occur in perfect periodic structures such as that illustrated in Fig. 15.2(b) and possible irregularities in the positions of the spin-slip planes. The former is in principle included in our calculations whereas the latter is not. From the calculated magnetic structures, such as those illustrated in Fig. 15.2, we could readily deduce the corresponding neutron-diffraction patterns and hence, by fitting the peak intensities, determine the values for α and σ which are shown as a function of b in Fig. 15.3. The parametrization suggested by Cowley and Bates is in practice rather satisfactory; it allows a fit of all the calculated neutron-diffraction intensities, which vary over about five orders of magnitude, with a relative error of in all cases of less than 20 per cent. Furthermore, as illustrated in Fig. 15.3, the parameter α is close to the average values of the angle ϕ determined directly from the calculated structures.

The measured and calculated values of α are in general agreement, taking into account the experimental uncertainties, but there are substantial discrepancies in σ . It is noteworthy that the agreement between the predicted and observed neutron-diffraction intensities is very good for the $b = 11$, one-spin-slip structure, and that the experimental values of σ otherwise lie consistently above the theoretical. This may indicate that the perfect periodicity of the less stable spin-slip structures is more effectively disturbed by imperfections.

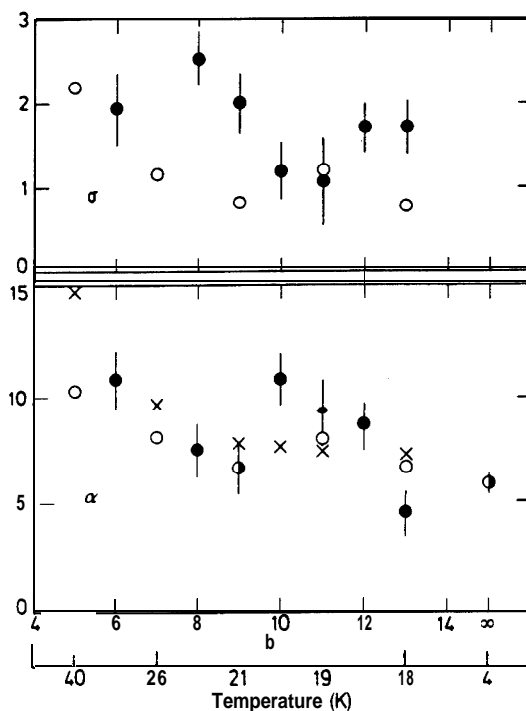


FIG. 15.3. The comparison between the neutron-diffraction measurements on spin-slip structures by Cowley and Bates (1988) (closed circles) and the calculations (open circles). In the lower figure, the parameter α which, in an undistorted structure, is half the mean angle between the moments in a bunched pair, is plotted against b , the number of lattice planes between spin-slips. The open circles show the values of α deduced from the calculated neutron-diffraction patterns, using an analysis similar to that of Cowley and Bates, while the crosses are the average bunching angles determined directly from the structures. In the upper figure, the experimental and calculated distortion parameters σ are compared. They agree for the stable one-spin-slip structure, but the experimental σ is greater for the others, indicating that they may not be perfectly periodic.

15.3. The magnetization process in holmium

The effect of a magnetic field applied in the plane of a helical structure was first discussed in detail by Nagamiya *et al.* (1962) on the basis of a mean-field model. As the field is increased, the helix first distorts to provide a moment along \mathbf{H} , and then undergoes a first-order transition to a fan structure, in which the moments oscillate about the field direction. A further increase in the field reduces the opening angle of the fan which, in the absence of magnetic anisotropy, goes continuously to zero, establishing a ferromagnetic phase at a second-order transition.

Hexagonal anisotropy may modify this process into a first-order transition or, if it is large enough, eliminate the fan phase entirely.

The magnetization curves of holmium measured by Strandburg *et al.* (1962) and Feron (1969) behaved in accordance with this description at low temperatures but, above about 40 K when the fan phase was first observed, a further phase also appeared, manifested by a plateau corresponding to a moment about one-half of that attained in the fan phase. This extra phase was clearly apparent in the magnetoresistance measurements of Mackintosh and Spanel (1964), and later experiments by Akhavan and Blackstead (1976), in which the field was changed continuously, revealed as many as five different phases at some temperatures. The structures in a magnetic field were investigated with neutron diffraction by Koehler *et al.* (1967), who identified two intermediate phases which they called fans and characterized by the intensity distribution of the Bragg peaks.

In order to elucidate these phenomena we have calculated the effect of a magnetic field on the commensurable structures of Fig. 15.2. At low temperatures the hexagonal anisotropy has a decisive influence on the magnetic structures, ensuring that a first-order transition occurs from the helix or cone to the ferromagnet, without any intermediate phases. Below about 20 K, where the cone is the stable structure in zero field, the cone angle is almost independent of the applied field but, at the transition to the ferromagnet, the *c*-axis moment disappears. When the field is applied in the hard direction at these temperatures, the moments just above the ferromagnetic transition do not point along the field direction but are aligned very closely with the nearest easy axis. As the field is further increased they turn towards it, becoming fully aligned through a second-order phase transition at a critical field which is estimated from B_0^6 to be about 460 kOe at absolute zero. At low temperatures, the hexagonal anisotropy also hinders the smooth distortion of the helix in a field. The moments jump discontinuously past the hard directions as the field is increased, giving first-order transitions which may have been observed, for example, as low-field phase boundaries below 20 K in the measurements of Akhavan and Blackstead (1976).

Above about 40 K, when the hexagonal anisotropy is not so dominant, intermediate stable phases appear between the helix and the ferromagnet. The nature of these phases may be appreciated by noting that the helix can be considered as blocks of moments with components alternately parallel and antiparallel to the field, as is apparent from the structures illustrated in Fig. 15.2. If we write this pattern schematically as (+ - + -), then the fan structure may be described as (++++). The new phases,

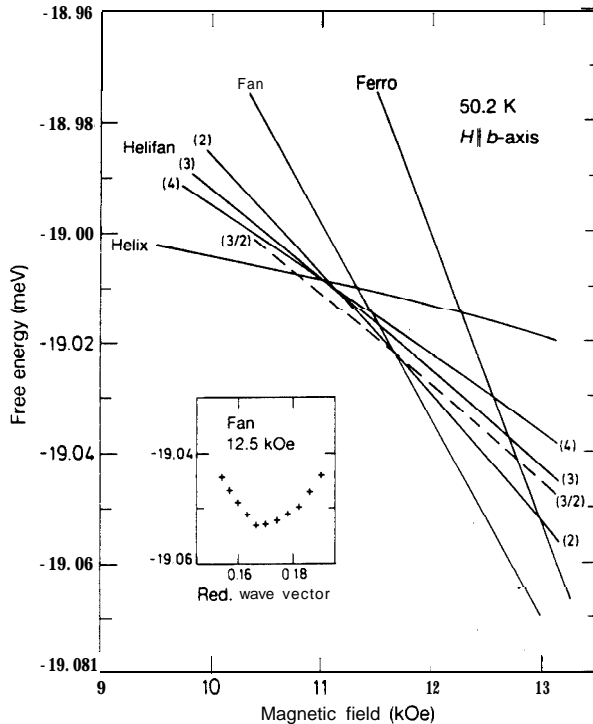


FIG. 15.5. The magnetic free energy for different magnetic structures in holmium at 50 K, as a function of the magnetic field along an easy b -axis. The free energy is in each case minimized with respect to the wave vector which characterizes the structure, as illustrated for the fan phase in the insert.

structures follow the sequence helix \rightarrow helifan(3/2) \rightarrow fan \rightarrow ferromagnet as the field is increased. The helifan(3/2) is depicted in Fig. 15.6. The various structures are associated with characteristic neutron-diffraction patterns, illustrated in Fig. 15.7. An examination of the neutron-diffraction intensities which Koehler *et al.* (1967) associate with the phase which they designate as 'Fan I' reveals a striking correspondence with the helifan(3/2) pattern, as shown by Jensen and Mackintosh (1990), with a very weak fundamental at $\mathbf{Q}_0/3$, where \mathbf{Q}_0 is approximately the wave vector of the helix, strong second and third harmonics, and a weak fourth harmonic. The basic periodicities of this structure are $2\mathbf{Q}_0/3$ for the component of the moments parallel to the field, and \mathbf{Q}_0 for the perpendicular component: the weak $\mathbf{Q}_0/3$ peak arises as the result of interference between them. Similar but more detailed neutron-diffraction results have recently been obtained by J. D. Axe, J. Bohr, and D. Gibbs (private communication). As may be seen from Fig 15.7, the changes in

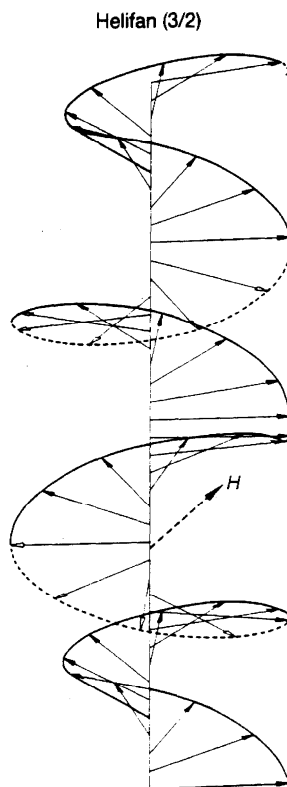


FIG. 15.6. The helifan(3/2) structure in holmium at 50 K. The moments lie in planes normal to the c -axis and their relative orientations are indicated by arrows. A magnetic field of 11 kOe is applied in the basal plane and moments with components respectively parallel and antiparallel to the field are designated by filled and open arrow-heads. This component of the moments has a periodicity which is $3/2$ that of the corresponding helix and the helicity of the structure changes regularly.

the basic wave vector are substantial, even though the underlying exchange function is constant, and they agree very well with those observed by neutron diffraction. For the helix, fan, and helifan(3/2) structures the experimental (theoretical) values of \mathbf{Q} are respectively 0.208 (0.211), 0.170 (0.168), and 0.063 (0.066), relative to the reciprocal lattice vector \mathbf{b}_3 . The period of the fan phase increases relative to that of the helix because of the resulting increase in the opening angle of the fan. This allows a decrease in the exchange energy which is greater than the concomitant increase of the Zeeman energy. The change in \mathbf{Q} in the various helifan phases is therefore, to a very good approximation, proportional to their magnetization.

Examples of the isothermal magnetization curves measured in holmium

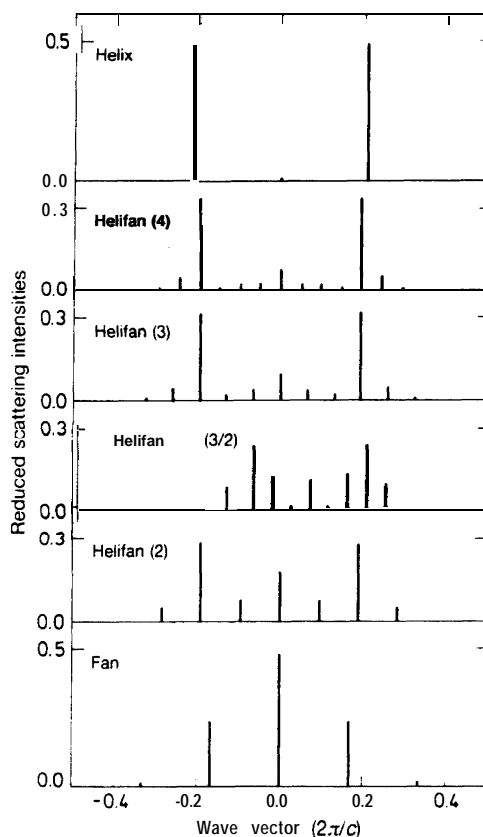


FIG. 15.7. The neutron diffraction patterns predicted for the different periodic structures at 50 K. The scattering vector is assumed to lie along the c -axis. The structures are calculated with a field of 11 kOe along the b -axis.

are shown in Fig. 15.8 and compared with the calculated results. A consideration of all the available magnetization data (Strandburg *et al.* 1962; Feron 1969) clearly reveals the presence of a plateau in the ordered moment between the helix and the fan phase, and the value of the intermediate moment is generally larger than that corresponding to the helifan(3/2) structure. This indicates that the metastable helifan(2) phase may replace or coexist with the stable (3/2)-structure in such magnetization measurements. The occurrence of phases which are not thermodynamically stable may be explained by a closer examination of the structures of Fig. 15.4. The helifan($n = \text{integer}$) configurations may all be derived from the helix by transforming one in n (-) blocks into (+) blocks. Since there are only odd numbers of adjacent (+) blocks,

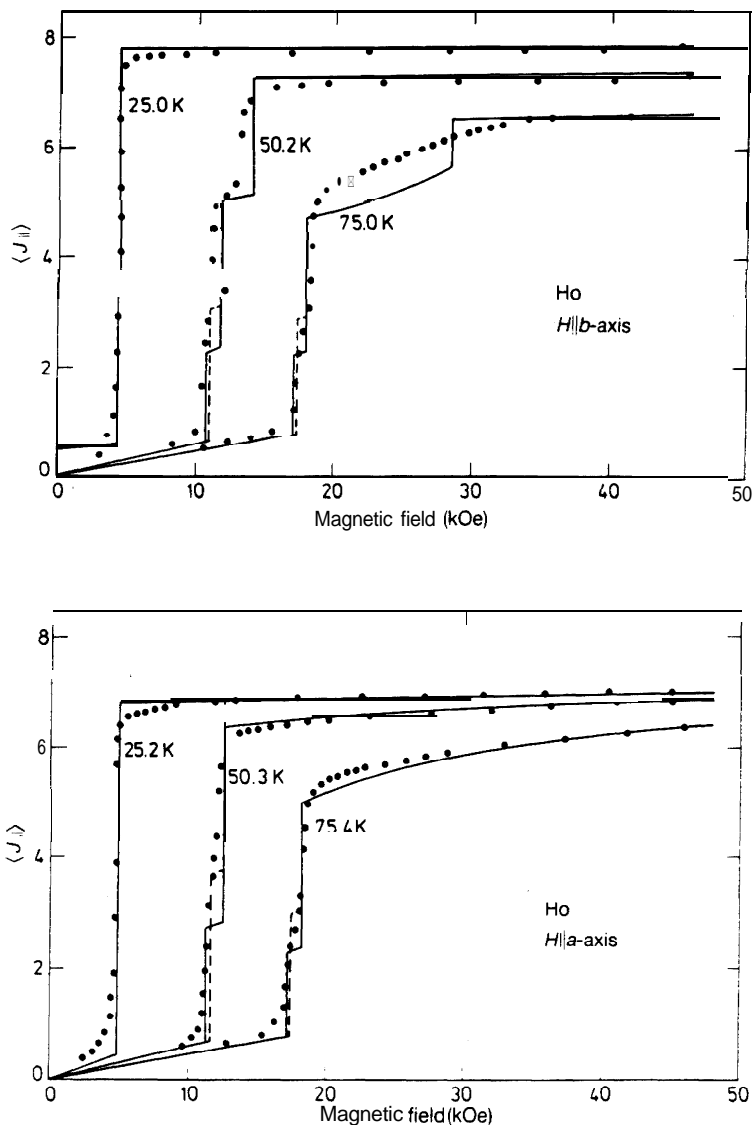


FIG. 15.8. The calculated magnetization of holmium (Ho) (given by $g\mu_B\langle J_{\parallel} \rangle$ per ion), compared with the experimental results of Feron (1969). In the upper figure the field is applied along the easy b -axis. At 50 K and 75 K the thermodynamically stable intermediate phase between the helix and the fan is the helifan(3/2). However the predicted moment for this structure is too small compared with the experimental value, and the metastable helifan(2) phase, whose magnetization is indicated by dashed lines, accounts at least as well for the magnitude of the moment measured over a range of temperatures in this intermediate phase. The difference in free energy between the fan and the ferromagnetic phase at 75 K is predicted to be very small

conserved. On the other hand, the helicity of the helical regions is generating the helifan(3/2) structure from the helix requires the metamorphosis of regularly spaced (- + -) blocks into (+ - +), and the helicities of neighbouring helical regions are reversed. We should expect that the energy barrier for such a complex process would be relatively high and therefore suggest that experiments such as neutron diffraction, which are performed at a fixed field over a long time-scale, detect the pure thermodynamically stable (3/2) phase, while a rapidly increasing field may induce metastable (n) domains. The helifan(2) structure has apparently been observed in the magnetization measurements, and other metastable helifans may be involved in the five phases observed by Akhavan and Blackstead (1976). In addition, the very pronounced hysteresis which they observed is consistent with the fact that the helifan(3/2) phase is readily formed from the fan in decreasing fields.

The stability of the helifan structures is determined by the form of the two-ion coupling, especially the long-range component. If the exchange is sufficiently short-range, the helix, helifans, and fan are almost degenerate at the critical field; it is the interaction between the blocks which differentiates between these structures. Helifans may also occur in other rare-earth systems, for example, dysprosium and erbium, where helical ordering is observed. It would clearly be of interest to explore the boundaries of the helifan region when the exchange is altered by temperature or alloying, and to examine the metastable helifan structures by neutron diffraction in a changing magnetic field.

15.4. Magnetic excitations

The magnetic excitations of commensurable periodic structures display a number of interesting features. If B_2^0 is positive and the other crystal-field parameters, including B_6^0 , are negligible, and $\mathcal{J}(\mathbf{q})$ is isotropic and has a maximum at some non-zero value \mathbf{Q} in the c -direction. the stable structure is a generally incommensurable planar helix. The excitations of this structure have been discussed, for example, by Mackintosh and Bjerrum Møller (1972) and the dispersion relation in the c -direction is

by 20 kOe (where it corresponds to a field of less than 2 kOe) and dipolar forces may smear out the predicted first-order transition between the two phases. as is indicated by the experimental results. The non-zero moment at 25 K in low fields is due to the net moment carried by the 11-layer one-spin-slip structure, which is stable at this temperature. In the lower figure the field is along the hard a -axis. The calculated magnetization curves at 25 K are for the helix and the ferromagnet, while at 50 and 75 K they are for the helix, the helifan(3/2), the helifan(2) (dashed), and the fan phase, which is stable to very high fields at these temperatures.

given by

$$\varepsilon(\mathbf{q}) = J \{ [\mathcal{J}(\mathbf{Q}) - \frac{1}{2}\mathcal{J}(\mathbf{q} + \mathbf{Q}) - \frac{1}{2}\mathcal{J}(\mathbf{q} - \mathbf{Q})] \cdot [\mathcal{J}(\mathbf{Q}) - \mathcal{J}(\mathbf{q}) + 6B_2^0] \}^{1/2},$$

measuring \mathbf{q} in a coordinate system which rotates about the c -axis with the helix. The invariance of the helix under such a rotation gives rise to a Goldstone mode, so that the excitation energy goes to zero with \mathbf{q} . Furthermore, the energy at $\mathbf{q} = \mathbf{Q}$ vanishes with the axial anisotropy, resulting in a soft mode which drives a second-order phase transition to a helical structure which is tilted out of the hexagonal plane (Elliott 1971; Sherrington 1972).

A large B_6^0 changes this picture drastically. If a commensurate or quasi-commensurate structure is formed, the excitations may readily be calculated by the random-phase approximation (Jensen 1988). From the self-consistent mean-field energies and eigenfunctions, the frequency-dependent susceptibility tensor $\bar{\chi}_0(i, \omega)$ is calculated for an ion in each layer of the periodic structure. The random-phase approximation (RPA) susceptibility tensor is then determined by

$$\bar{\chi}(ij, \omega) = \bar{\chi}_0(i, \omega)\delta_{ij} + \sum \bar{\chi}_0(i, \omega)\bar{\mathcal{J}}(ij')\bar{\chi}(j'j, \omega).$$

These equations are transformed into a coordinate system rotating with the moments, and a subsequent Fourier transformation gives $\bar{\chi}(\mathbf{q}, \omega)$. The imaginary part of this function is proportional to the inelastic neutron scattering cross-section, whose peaks define the excitation energies.

Experimental studies of these excitations are so far relatively sparse. The zero-spin-slip structure of Fig. 15.2(a) has been examined in some detail by neutron scattering by Larsen *et al.* (1987), who used a crystal of holmium containing 10 per cent of terbium (Tb) in order to stabilize the commensurate 12-layer helix. Their results for both the ferromagnetic and helical phases are shown in Fig. 15.9. In contrast to the incommensurate case, the commensurate helix has translational symmetry along the c -axis, and an energy gap occurs at long wavelengths, reflecting the force necessary to turn the bunched moments away from the easy directions of magnetization. The difference in the magnitude of this gap between the ferromagnetic and helical phases is an indication of an anisotropic two-ion coupling. The discontinuities in the dispersion relations at $\mathbf{q} = \mathbf{0}$ are due to the dipolar interaction which, though weak, is of long range and highly anisotropic. These characteristics allow it to stabilize the cone structure, rather than the tilted helix, in holmium at low temperatures. Correspondingly, the soft mode of the helix is not that at \mathbf{Q} , but rather the lower of the dipolar-split modes at the origin, which

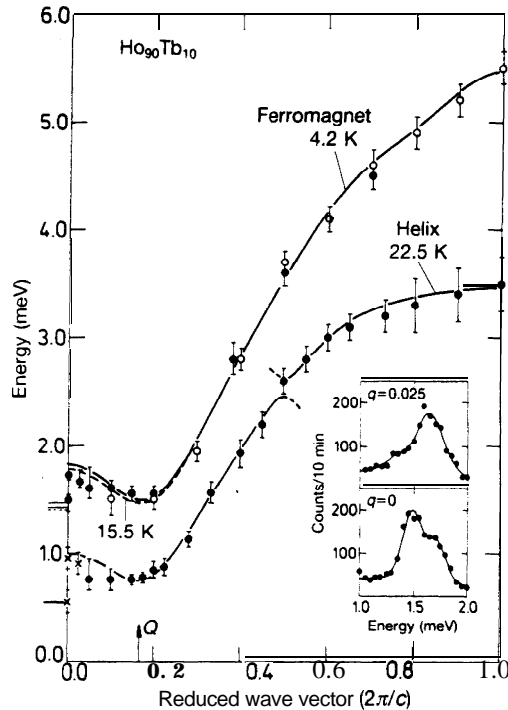


FIG. 15.9. Dispersion relations for the magnetic excitations propagating in the c -direction of $\text{Ho}_{90}\text{Tb}_{10}$. The upper branch is for the ferromagnetic phase. The calculated long-wavelength energies in the basal plane are shown to the left of the ordinate axis, and the discontinuity due to the dipolar interaction is clearly manifested in the experimental measurements, shown in the insert. The lower curve is for the commensurable helical structure. The calculated small energy gap at the centre of this branch, which is due to the bunching, is not resolved experimentally.

gives rise to the ferromagnetic component of the cone when its energy falls to zero.

The calculated small energy gap at the centre of the branch in the commensurable helix is due to the bunching of the moments illustrated in Fig. 15.2(a), which doubles the periodicity in the rotating coordinate system and thereby halves the Brillouin zone in the c direction. This gap is considerably smaller than the experimental energy resolution, and it is therefore not surprising that it was not observed. The equivalent gap has however been measured in the one-spin-slip structure of Fig. 15.2(b) by Patterson *et al.* (1990), as illustrated in Fig. 15.10. In this case the 11-layer structure causes an 11-fold reduction in the Brillouin zone, but only the first-order gap at $5/11$ of the original zone boundary is calculated to be observable. This gap, on the other hand, is considerably amplified,

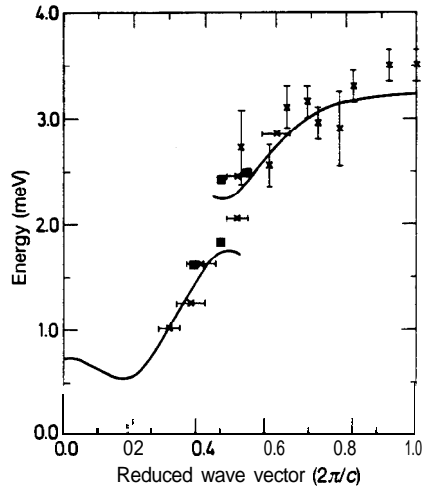


FIG.15.10. The dispersion relation for the excitations propagating in the c -direction in the one-spin-slip structure of holmium at 20 K. The full curve is the calculation of Jensen (1988). The crosses are the experimental results of Stringfellow *et al.* (1970), and the squares those of Patterson *et al.* (1990). In these measurements the energy gap at $q = \frac{5}{11}(2\pi/c)$, is resolved.

as compared to that in the structure without spin slips. As the number of spin slips increases the corresponding excitation spectra, which have been calculated by Jensen (1988), become more complex. The trigonal structure of Fig. 15.2(d), for example, has three branches of excitations, while the dispersion relation for the structure of Fig. 15.2(c) is broken into short segments by a succession of energy gaps. Because of this increasing complexity, together with the broadening of the excitations and the decreasing stability of the spin-slip structures, the dispersion relations become rapidly more difficult to study with increasing temperature, and identifying those features which depend on the large value of B_6^0 becomes concomitantly uncertain.

Nevertheless, even at temperatures above about 50 K, when $\langle O_6^0 \rangle$ in holmium is small and the distortion of the helix correspondingly weak, the exceptionally large B_6^0 still plays an important role by mixing the otherwise pure $|J_z\rangle$ molecular-field (MF) states. Indeed, as the temperature is increased and the MF decreases this effect becomes relatively more important so that, for example, the energy difference between the two lowest MF levels varies by an order of magnitude as the moment on the site moves from an easy to a hard direction at elevated temperatures. While this variation is much smaller in the low-temperature limit. The large changes in the MF states from site to site tend to disrupt

the coherent propagation of the collective modes, providing a mechanism for the creation of energy gaps in the excitation spectrum.

When the moments are not along a direction of high symmetry, B_0^6 also mixes the transverse and longitudinal components of the single-site susceptibility, so that the normal modes are no longer either pure transverse spin waves or longitudinal excitations. At low temperatures, where $\langle J_z \rangle$ is close to its maximum value, this mixing is unimportant, but it has significant effects on the excitations at higher temperatures. In the RPA the longitudinal response contains an elastic component, and the excitation spectrum in the long-wavelength limit therefore comprises an elastic and an inelastic branch. The inelastic mode is calculated to lie around 1 meV in the temperature interval 50-80 K. In the RPA this feature is independent of whether the magnetic periodicity is commensurate with the lattice. In the incommensurate case the invariance of the helix under rotation about the c -axis is not reflected in a conventional Goldstone mode, since the corresponding generator of rotations does not commute with the O_6^6 term in the Hamiltonian. This symmetry is rather manifested in the elastic, zero-energy phason mode, which coexists with an inelastic phason. This situation is entirely equivalent to that found in the longitudinally ordered phase of praseodymium (Jensen *et al.* 1987). Beyond the RPA the elastic response is smeared out into a diffusive mode of non-zero width. As in praseodymium this broadening may essentially eliminate the inelastic phason mode, leaving only a diffusive peak centred at zero energy in the long-wavelength limit. The width of this peak goes to zero at the magnetic Bragg reflection, and true inelastic mode only appears some distance away.

In the calculations of Jensen (1988) the elastic single-site response was assumed to be broadened by about 6 meV, corresponding to the spin-wave bandwidth. This assumption gives a reasonable account of the excitations in the long-wavelength limit, suggesting that they become overdamped if the wave vector is less than about one-tenth of the extension of the zone. Although the inelastic phason mode is largely eliminated, the calculations suggest that a residue may be observable. The most favourable conditions for detecting it would occur in a neutron-scattering scan with a large component of the scattering vector in the basal plane at about 40 K.

Acknowledgement

As may be deduced from the acknowledgements in the articles on rare-earth metals to which we have contributed, Roger Elliott has given

vital support to our research, through his knowledge of the field and his willingness to use his insight to help others. It is therefore a great pleasure for us to contribute to this volume and to reiterate our gratitude to him for countless useful discussions through the years.

References

- Akhavan, M. and Blackstead, H. A. (1976). *Physical Review*, **B13**, 1209.
- Cooper, B. R., Elliott, R. J., Nettel, S. J., and Suhl, H. (1962). *Physical Review*, **127**, 57.
- Cowley, R. A. and Bates, S. B. (1988). *Journal of Physics*, **C21**, 4113.
- Elliott, R. J. (1961). *Physical Review*, **124**, 346.
- Elliott, R. J. (1971). *Atomic Energy of Canada Limited Report*. No. 3805.
- Feron, J. L. (1969). Unpublished D.Phil. thesis, University of Grenoble. (See also Coqblin, B. (1977). *The electronic structure of rare-earth metals and alloys: the magnetic heavy rare-earths*, Figs 198 and 199. Academic Press, London.)
- Gibbs, D., Moncton, D. E., D'Amico, K. L., Bohr, J., and Grier, B. H. (1985). *Physical Review Letters*, **55**, 234.
- Jensen, J. (1976). *Journal of Physics*, **F6**, 1145.
- Jensen, J. (1988). *Journal de Physique (Paris)*, **49** (C8), 351.
- Jensen, J., McEwen, K. A., and Stirling, W. G. (1987). *Physical Review*, **B35**, 3327.
- Jensen, J. and Mackintosh, A. R. (1990). *Physical Review Letters*, **64**, 2699.
- Koehler, W. C., Cable, J. W., Child, H. R., Wilkinson, M. K., and Wollan, E. O. (1967). *Physical Review*, **158**, 450.
- Larsen, C. C., Jensen, J., and Mackintosh, A. R. (1987). *Physical Review Letters*, **59**, 712.
- Mackintosh, A. R. and Bjerrum Møller, H. (1972). In *Magnetic properties of rare earth metals* (ed. R. J. Elliott), p. 187. Plenum. London.
- Mackintosh, A. R. and Spanel, L. E. (1964). *Solid State Communications*, **2**, 383.
- Nagamiya, T., Nagata, K., and Kitano, Y. (1962). *Progress in Theoretical Physics (Kyoto)*, **27**, 1253.
- Patterson, C., McMorrow, D. F., Godfrin, H., Clausen, K. F., and Lebeck, B. (1990). *Journal of Physics: Condensed Matter*, **2**, 3421.
- Sherrington, D. (1972). *Physical Review Letters*, **28**, 364.
- Strandburg, D. L., Legvold, S., and Spedding, F. H. (1962). *Physical Review*, **127**, 2046.
- Stringfellow, M. W., Holden, T. M., Powell, B. M., and Woods, A. D. B. (1970). *Journals of Physics*, **C3**, S 189.